Topological Derivative를 이용한 선형 구조물의 레벨셋 기반 형상 최적 설계

Level Set Based Shape Optimization of Linear Structures Using Topological Derivatives

하 승 현* · 김 민 근* · 조 선 호**

Ha, Seung-Hyun · Kim, Min-Geun · Cho, Seon-Ho

ABSTRACT

Using a level set method and topological derivatives, a topological shape optimization method that is independent of an initial design is developed for linearly elastic structures. In the level set method, the initial domain is kept fixed and its boundary is represented by an implicit moving boundary embedded in the level set function, which facilitates to handle complicated topological shape changes. The "Hamilton-Jacobi (H-J)" equation and computationally robust numerical technique of "up-wind scheme" lead the initial implicit boundary to an optimal one according to the normal velocity field while minimizing the objective function of compliance and satisfying the constraint of allowable volume. Based on the asymptotic regularization concept, the topological derivative is considered as the limit of shape derivative as the radius of hole approaches to zero. The required velocity field to update the H-J equation is determined from the descent direction of Lagrangian derived from optimality conditions. It turns out that the initial holes is not required to get the optimal result since the developed method can create holes whenever and wherever necessary using indicators obtained from the topological derivatives. It is demonstrated that the proper choice of control parameters for nucleation is crucial for efficient optimization process.

Keywords: *Shape design optimization, Topological derivative, Level set method, Adjoint sensitivity analysis*

1. LEVEL SET METHOD

Let $\Omega \subset R^d$ be a bounded open domain with a smooth boundary Γ as shown in Figure 1.

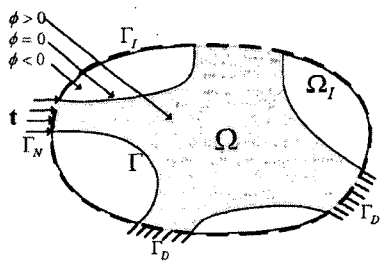

Figure 1 Level set function

Imagine the boundary Γ of the domain moves in the direction normal to its boundary with a given speed V_n. To derive the equation of moving boundary as time evolves, we regard this propagating boundary as the zero level set $\phi(\mathbf{x}, \tau = 0)$ of a (d+1)-dimensional function $\Phi(\phi, k)$. At time $\tau = 0$, assume the existence of a zero level set function $\phi(\mathbf{x}, 0)$ that is Lipschitz continuous and defined on Ω_I, satisfying

* 학생회원, 서울대학교 조선해양공학과 박사과정

** 정회원, 서울대학교 조선해양공학과 및 해양시스템공학연구소(RIMSE) 교수

$$\phi(\mathbf{x},\tau=0)\begin{cases}+\zeta(\mathbf{x},\Gamma) & \mathbf{x}\in\Omega \\ =0 & \mathbf{x}\in\Gamma \\ -\zeta(\mathbf{x},\Gamma) & \mathbf{x}\in\Omega_I\setminus\overline{\Omega}\end{cases} \tag{1}$$

where $\zeta(\mathbf{x},\Gamma)$ is a distance function from a point $\mathbf{x}$ to the boundary Γ, for all $\mathbf{x}\in R^d$. Γ_I represents an initial reference boundary. Ω_I denotes an initial reference domain that includes all the possible domains Ω as

$$\Omega\subseteq\Omega_I. \tag{2}$$

Using the level set function ϕ, an outward unit vector $\mathbf{n}$ normal to the boundary Γ is obtained by

$$\mathbf{n}=-\frac{\nabla\phi}{|\nabla\phi|} \tag{3}$$

and a curvature κ is defined as the divergence of $\mathbf{n}$

$$\kappa=div\,\mathbf{n}=-\nabla\cdot\left(\frac{\nabla\phi}{|\nabla\phi|}\right). \tag{4}$$

Consider a two dimensional level set function ϕ for the simplicity of problems. We employ the level set method for the implicit representation of moving boundaries. The level set model describes a boundary in implicit form at zero level as the iso-surface of a scalar function $\phi: R^2\rightarrow R$ embedded in three dimensional space.

$$S=\{\mathbf{x}:\phi(\mathbf{x},0)=k\}, \tag{5}$$

where k and $\mathbf{x}$ are an arbitrary iso-value and a point on the iso-surface ϕ, respectively. Taking the material derivative of level set function with respect to a perturbation parameter τ leads to the "Hamilton-Jacobi Equation" as

$$\begin{aligned}\frac{D\phi}{D\tau}&\equiv\frac{\partial\phi(\mathbf{x}_\tau,\tau)}{\partial\tau}\bigg|_{\tau=0}+\nabla\phi(\mathbf{x}_\tau,\tau)|_{\tau=0}\cdot\frac{d\mathbf{x}_\tau}{d\tau}\bigg|_{\tau=0}\\&=\frac{\partial\phi(\mathbf{x},0)}{\partial\tau}+\nabla\phi(\mathbf{x},0)\cdot\frac{d\mathbf{x}}{d\tau}=0.\end{aligned} \tag{6}$$

Let V_n be a speed function normal to the boundary. Using Equation (3), we have the following.

$$V_n=\mathbf{V}\cdot\mathbf{n}=-\mathbf{V}(\mathbf{x})\cdot\frac{\nabla\phi}{|\nabla\phi|}. \tag{7}$$

Using Equations (7) and applying appropriate boundary conditions, Equation (6) is rewritten as

$$\frac{\partial\phi}{\partial\tau}=V_n|\nabla\phi|,\quad\frac{\partial\phi}{\partial n}\bigg|_{\Gamma_I}=0. \tag{8}$$

2. ELASTICITY PROBLEMS

Consider an equilibrium equation for elasticity problems on a generic domain Ω,

$$\nabla\cdot\boldsymbol{\sigma}+\mathbf{b}=\mathbf{0},\quad\mathbf{x}\in\Omega, \tag{9}$$

where $\mathbf{b}$ is a body force intensity. Dirichlet and Neumann boundary conditions are respectively imposed as

$$\mathbf{z}=\mathbf{0},\quad\mathbf{x}\in\Gamma_D\quad\text{and}\quad\boldsymbol{\sigma}\cdot\mathbf{n}=\mathbf{t},\quad\mathbf{x}\in\Gamma_N. \tag{10}$$

Also, strain-displacement and constitutive relations are defined, respectively, as

$$\boldsymbol{\varepsilon}=\frac{1}{2}(\nabla\mathbf{z}+\nabla\mathbf{z}^T)\ \text{and}\ \boldsymbol{\sigma}=\mathbf{C}:\boldsymbol{\varepsilon}. \tag{11}$$

where $\mathbf{C}$ is the elastic material response tensor. Using a virtual displacement $\bar{\mathbf{z}} \in Z$, a variational equation can be written as

$$a(\mathbf{z},\bar{\mathbf{z}}) \equiv \int_\Omega \boldsymbol{\varepsilon}(\mathbf{z}) : \mathbf{C} : \boldsymbol{\varepsilon}(\bar{\mathbf{z}}) d\Omega = \int_\Omega \mathbf{b}\cdot\bar{\mathbf{z}} d\Omega + \int_{\Gamma_N} \mathbf{t}\cdot\bar{\mathbf{z}} d\Gamma \equiv \ell(\bar{\mathbf{z}}), \quad \forall \bar{\mathbf{z}} \in Z, \tag{12}$$

where

$$Z = \left\{ \mathbf{z} \in \left[H^1(\Omega)\right]^d : \mathbf{z} = \mathbf{0} \quad on \quad \Gamma_D \right\}. \tag{13}$$

To derive an adjoint equation for the variational equation (12), consider a general performance functional $\psi(\mathbf{z})$ as

$$\psi(\mathbf{z}) = \int_\Omega F(\mathbf{z}) d\Omega . \tag{14}$$

Taking the Fréchet derivative $\langle \bullet, \bullet \rangle$ with respect to $\mathbf{z}$ in the direction of $\bar{\mathbf{z}}$ leads to

$$\left\langle \frac{\partial \psi(\mathbf{z})}{\partial \mathbf{z}}, \bar{\mathbf{z}} \right\rangle = \int_\Omega \frac{\partial F(\mathbf{z})}{\partial \mathbf{z}} \bar{\mathbf{z}} d\Omega . \tag{15}$$

Define a Lagrangian, using Equation (12), as

$$L(\mathbf{z},\boldsymbol{\lambda}) = \psi(\mathbf{z}) - a(\mathbf{z},\boldsymbol{\lambda}) + \ell(\boldsymbol{\lambda}), \quad \forall \boldsymbol{\lambda} \in Z, \tag{16}$$

where $\boldsymbol{\lambda}$ is the solution of an adjoint system. Taking the Fréchet derivative of Equation (16) with respect to $\mathbf{z}$ in the direction of $\bar{\boldsymbol{\lambda}}$ and using a stationary condition, the adjoint equation can be derived as

$$\left\langle \frac{\partial}{\partial \mathbf{z}} L(\mathbf{z},\boldsymbol{\lambda}), \bar{\boldsymbol{\lambda}} \right\rangle = \left\langle \frac{\partial}{\partial \mathbf{z}} \psi(\mathbf{z}), \bar{\boldsymbol{\lambda}} \right\rangle - \left\langle \frac{\partial}{\partial \mathbf{z}} a(\mathbf{z},\boldsymbol{\lambda}), \bar{\boldsymbol{\lambda}} \right\rangle = 0 . \tag{17}$$

Thus, the abstract form of the adjoint system can be defined as

$$a(\boldsymbol{\lambda},\bar{\boldsymbol{\lambda}}) \equiv \left\langle \frac{\partial}{\partial \mathbf{z}} a(\mathbf{z},\boldsymbol{\lambda}), \bar{\boldsymbol{\lambda}} \right\rangle = \left\langle \frac{\partial \psi(\mathbf{z})}{\partial \mathbf{z}}, \bar{\boldsymbol{\lambda}} \right\rangle \equiv \ell(\bar{\boldsymbol{\lambda}}), \quad \forall \bar{\boldsymbol{\lambda}} \in Z . \tag{18}$$

3. SHAPE DERIVATIVE OF ELASTICITY

Using Equations (12), (14), and (16), define a Lagrangian for the compliance functional of elasticity problems as

$$L(\mathbf{z},\boldsymbol{\lambda}) = \int_\Omega \mathbf{b}\cdot\mathbf{z} d\Omega + \int_{\Gamma_N} \mathbf{t}\cdot\mathbf{z} d\Gamma - \int_\Omega \boldsymbol{\varepsilon}(\mathbf{z}) : \mathbf{C} : \boldsymbol{\varepsilon}(\boldsymbol{\lambda}) d\Omega + \int_\Omega \mathbf{b}\cdot\boldsymbol{\lambda} d\Omega + \int_{\Gamma_N} \mathbf{t}\cdot\boldsymbol{\lambda} d\Gamma, \quad \forall \boldsymbol{\lambda} \in Z, \tag{19}$$

where $\boldsymbol{\lambda}$ is the solution of the following adjoint equation,

$$a(\boldsymbol{\lambda},\bar{\boldsymbol{\lambda}}) = \int_\Omega \mathbf{b}\cdot\bar{\boldsymbol{\lambda}} \Omega + \int_{\Gamma_N} \mathbf{t}\cdot\bar{\boldsymbol{\lambda}} d\Gamma, \quad \forall \bar{\boldsymbol{\lambda}} \in Z . \tag{20}$$

Likewise, for the perturbed design, we have the following.

$$L_\tau(\mathbf{z}_\tau,\boldsymbol{\lambda}_\tau) = \int_{\Omega_\tau} \mathbf{b}\cdot(\mathbf{z}_\tau + \boldsymbol{\lambda}_\tau) d\Omega_\tau + \int_{\Gamma_{N_\tau}} \mathbf{t}\cdot(\mathbf{z}_\tau + \boldsymbol{\lambda}_\tau) d\Gamma_\tau - \int_{\Omega_\tau} \boldsymbol{\varepsilon}(\mathbf{z}_\tau) : \mathbf{C} : \boldsymbol{\varepsilon}(\boldsymbol{\lambda}_\tau) d\Omega_\tau, \quad \forall \boldsymbol{\lambda}_\tau \in Z_\tau, \tag{21}$$

where $\boldsymbol{\lambda}_\tau \equiv \boldsymbol{\lambda}(\mathbf{x}_\tau)$ is the solution of the following adjoint equation in the perturbed domain,

$$a_\tau(\boldsymbol{\lambda}_\tau,\bar{\boldsymbol{\lambda}}_\tau) = \int_{\Omega_\tau} \mathbf{b}\cdot\bar{\boldsymbol{\lambda}}_\tau \Omega_\tau + \int_{\Gamma_{N_\tau}} \mathbf{t}\cdot\bar{\boldsymbol{\lambda}}_\tau d\Gamma_\tau, \quad \forall \bar{\boldsymbol{\lambda}}_\tau \in Z_\tau . \tag{22}$$

Taking the shape derivative of Equation (21) in the direction of $\mathbf{V}$, we have the following.

$$\begin{aligned} \dot{L}_S(\mathbf{z},\boldsymbol{\lambda}) &= \int_\Omega \nabla\cdot\left[\left\{\mathbf{b}\cdot(\mathbf{z}+\boldsymbol{\lambda}) + \mathbf{t}\cdot\left(\nabla(\mathbf{z}+\boldsymbol{\lambda})\cdot\mathbf{n}\right) + \kappa\left(\mathbf{t}\cdot(\mathbf{z}+\boldsymbol{\lambda})\right) - \boldsymbol{\varepsilon}(\mathbf{z}) : \mathbf{C} : \boldsymbol{\varepsilon}(\boldsymbol{\lambda})\right\}\mathbf{V}\right] d\Omega \\ &= \int_\Omega \nabla\cdot\left\{\Pi(\mathbf{z},\boldsymbol{\lambda})\mathbf{V}\right\} d\Omega . \end{aligned} \tag{23}$$

4. TOPOLOGICAL DERIVATIVE OF PLANE ELASTICITY

Consider the various domains shown in Figure 2.

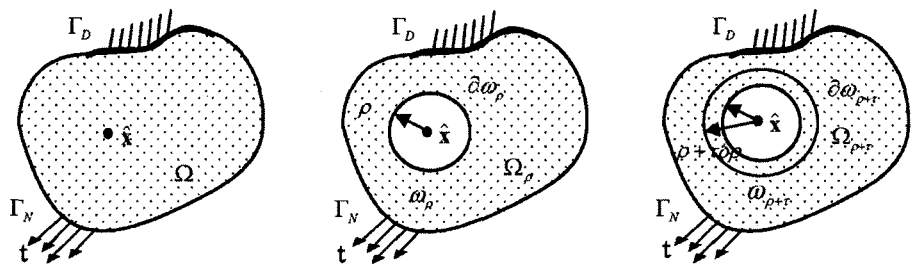

(a) Original domain (b) Topological variation (c) Shape variation

Figure 2 Various domains and variations

For the perturbed point $\mathbf{x}_\tau \in \partial\omega_{\rho+\tau}$ and the original point $\mathbf{x} \in \partial\omega_\rho$ on the line between $\mathbf{x}_\tau$ and the center of hole $\hat{\mathbf{x}} \in \omega_{\rho+\tau}$, the following relation holds.

$$\|\mathbf{x}_\tau - \mathbf{x}\| = \|\tau V_n \mathbf{n}\| = \tau\delta\rho \ . \tag{24}$$

Since $V_n < 0$ and $\delta\rho > 0$ when the hole is expanding,

$$\delta\rho = \|V_n \mathbf{n}\| = -V_n \ \text{ on } \ \partial\omega_\rho \ . \tag{25}$$

Taking the Lebesque measure as

$$|\omega_\rho| = -\int_{\omega_\rho} d\omega_\rho \ , \tag{26}$$

its derivative is obtained by

$$|\omega_\rho|_{,\tau} = -\frac{d}{d\tau}\int_{\omega_{\rho+\tau}} d\omega_{\rho+\tau}\Big|_{\tau=0} = \int_{\partial\omega_\rho} V_n d\partial\omega_\rho \ . \tag{27}$$

If a circular domain is selected, the variation of Lebesque measure is expressed as

$$\delta|\omega_\rho| = -2\pi\rho\delta\rho = 2\pi\rho V_n \ \text{ on } \ \partial\omega_\rho \ . \tag{28}$$

The corresponding shape derivative in boundary integral form is derived as

$$\dot{L}_S(\mathbf{z}_\rho, \boldsymbol{\lambda}_\rho) = \int_{\partial\omega_\rho} \Pi(\mathbf{z}_\rho, \boldsymbol{\lambda}_\rho) V_n d\Gamma_\rho \tag{29}$$

Note that since only the boundary of hole is perturbed, the design velocity vanishes on the other boundary. The topological derivative for the compliance is written as

$$\dot{L}_T(\mathbf{z}, \boldsymbol{\lambda})(\hat{\mathbf{x}}) = \lim_{\rho\to 0} \frac{1}{|\omega_\rho|_{,\tau}} \dot{L}_S(\mathbf{z}_\rho, \boldsymbol{\lambda}_\rho) \ , \ \ \forall \hat{\mathbf{x}} \in \Omega \ . \tag{30}$$

Using Equations (27) and (29), Equation (30) can be rewritten as

$$\dot{L}_T(\mathbf{z}, \boldsymbol{\lambda})(\hat{\mathbf{x}}) = \lim_{\rho\to 0} \frac{1}{\int_{\partial\omega_\rho} V_n d\partial\omega_\rho} \int_{\partial\omega_\rho} \Pi(\mathbf{z}_\rho, \boldsymbol{\lambda}_\rho) V_n d\Gamma_\rho \ , \ \ \forall \hat{\mathbf{x}} \in \Omega \ . \tag{31}$$

Since the traction vanishes on the boundary of hole $\partial\omega_\rho$, Equation (31) is rewritten as

$$\dot{L}_T(\mathbf{z}, \boldsymbol{\lambda})(\hat{\mathbf{x}}) = \lim_{\rho\to 0} \frac{1}{\int_{\partial\omega_\rho} V_n d\partial\omega_\rho} \int_{\partial\omega_\rho} \left\{ \mathbf{b}_\rho \cdot (\mathbf{z}_\rho + \boldsymbol{\lambda}_\rho) - \boldsymbol{\sigma}(\mathbf{z}_\rho) : \boldsymbol{\varepsilon}(\boldsymbol{\lambda}_\rho) \right\} V_n \partial\omega_\rho \ , \ \ \forall \hat{\mathbf{x}} \in \Omega \ . \tag{32}$$

Using asymptotic expansion, Equation (32) can be rewritten as

$$\dot{L}_T(\mathbf{z}, \boldsymbol{\lambda})(\hat{\mathbf{x}}) = -\eta\left[4\boldsymbol{\sigma}(\mathbf{z}) : \boldsymbol{\sigma}(\boldsymbol{\lambda}) - tr\boldsymbol{\sigma}(\mathbf{z}) tr\boldsymbol{\sigma}(\boldsymbol{\lambda})\right] \equiv -\Sigma(\mathbf{z}, \boldsymbol{\lambda})(\hat{\mathbf{x}}) \ , \tag{33}$$

where for the plane strain problems,

$$\Sigma(\mathbf{z}, \boldsymbol{\lambda})(\hat{\mathbf{x}}) = \frac{\lambda + 2\mu}{8\mu(\lambda + \mu)}\left[4\mu\boldsymbol{\sigma}(\mathbf{z}) : \boldsymbol{\varepsilon}(\boldsymbol{\lambda}) + (\lambda - \mu) tr\boldsymbol{\sigma}(\mathbf{z}) tr\boldsymbol{\varepsilon}(\boldsymbol{\lambda})\right] \tag{34}$$

and for the plane stress problems,

$$\Sigma(\mathbf{z},\boldsymbol{\lambda})(\hat{\mathbf{x}}) = \frac{\lambda+\mu}{\mu(3\lambda+2\mu)}\left[8\mu\boldsymbol{\sigma}(\mathbf{z}):\boldsymbol{\varepsilon}(\boldsymbol{\lambda}) + \frac{2\mu(\lambda-2\mu)}{(\lambda+2\mu)} tr\boldsymbol{\sigma}(\mathbf{z}) tr\boldsymbol{\varepsilon}(\boldsymbol{\lambda})\right] \tag{35}$$

λ, μ are Lamé constants, respectively.

5. TOPOLOGICAL SHAPE OPTIMIZATION

Formulation of Optimization Problems

The objective of topological shape optimization is to find the optimal layout that minimizes the compliance of system under prescribed loadings. Considering the domain and boundary before nucleation, the topological shape optimization problem is stated as

$$\text{Minimize } \psi = \int_{\Omega} \mathbf{b}\cdot\mathbf{z}d\Omega + \int_{\Gamma_N} \mathbf{t}\cdot\mathbf{z}d\Gamma, \tag{36}$$

$$\text{Subject to } m = \int_{\Omega} d\Omega \le M_{\max}, \tag{37}$$

where $M_{\max}$ is an allowable volume. The adjoint shape and topological derivatives of compliance in Equation (36) are readily available in Equations (23) and (33), respectively. Also, the shape derivative of Equation (37) is obtained by

$$\dot{m}_S = \left.\frac{dm_{\rho+\tau}}{d\tau}\right|_{\substack{\tau=0\\ \rho=0}} = \int_{\Omega} \nabla\cdot\mathbf{V}d\Omega \tag{38}$$

and the topological derivative by

$$\dot{m}_T(\hat{\mathbf{x}}) = \lim_{\rho\to 0}\frac{1}{|\omega_\rho|_\tau}\left.\frac{dm_{\rho+\tau}}{d\tau}\right|_{\tau=0} = 1. \tag{39}$$

The velocity field $\mathbf{V}(\mathbf{x})$ defines the propagation speed of all level sets along the outward normal direction. The velocity should be determined such that it reduces the compliance of system while satisfying the requirement of allowable material volume. Define a Lagrangian function Λ for the constrained optimization problems as

$$\Lambda(\tau,\mu,s) = \psi + \mu\left\{m + s^2 - M_{\max}\right\}, \tag{40}$$

where $M_{\max}$, s, and μ are the allowable material volume, a slack variable to convert the inequality constraint to the equality one, and a Lagrange multiplier, respectively. Using Kuhn-Tucker optimality conditions, the optimality condition is obtained to

$$\left.\frac{d\Lambda(\tau,\xi,s)}{d\tau}\right|_{\tau=0} = \int_{\Omega}\nabla\cdot\left\{\Pi(\mathbf{z},\boldsymbol{\lambda}) + \xi\right\}\mathbf{n}V_n d\Omega = 0, \tag{41}$$

where

$$\xi = \begin{cases} 0 & \text{if } \int_{\Omega} d\Omega < M_{\max} \\ \mu & \text{if } \int_{\Omega} d\Omega \ge M_{\max} \end{cases} \tag{42}$$

Velocity Computation

Now that the distance function $\phi(\mathbf{x})$ is normal to the boundary and the only normal velocity has influence on the result of shape optimization, the domain variation can be expressed, using the normal velocity $V_n(x)$.

$$\Omega_\tau = (\mathbf{I}d + \tau V_n)(\Omega_I). \tag{43}$$

Using Taylor series expansion in the normal direction of velocity field, the perturbed Lagrangian function

can be expressed as

$$\Lambda(\Omega_\tau)=\Lambda\{(\mathbf{I}d+\tau V_n)(\Omega_I)\}=\Lambda(\Omega_I)+\Lambda'(\Omega_I)(\tau V_n)+\cdots, \tag{44}$$

where the sensitivity of the Lagrangian function is expressed as

$$\Lambda'(\Omega_I)=\int_{\Omega_I}\delta(\phi)\{\Xi_\phi(e,\lambda)+\xi\}\varphi d\Omega. \tag{45}$$

If we take the boundary variation in the descent direction of the sensitivity as

$$V_n=-\{\Xi_\phi(e,\lambda)+\xi\}\varphi, \tag{46}$$

then the Equation (46) can be written as

$$\Lambda(\Omega_\tau)=\Lambda(\Omega_I)-\tau\int_{\Omega_I}\delta(\phi)\{\Xi(e,\lambda)+\xi\}^2\varphi^2 d\Omega+O(\tau^2)+\cdots, \tag{47}$$

Thus, the decrease of generalized compliance functional is guaranteed while satisfying the requirement of allowable material volume.

6. NUMERICAL EXAMPLES

Example 1: Topological sensitivity

The purpose of this example is to verify the derived topological sensitivity expressions. The verification model is shown in Figure 3-(a), where the plane model has the dimension of 2,430mm × 2,430mm, the thickness of 10mm, the Young's modulus of $E=2$ GPa, and the Poisson's ratio of $\nu=0.3$ for plane stress problems. The structure is subjected to a distributed load of $P_x=P_y=2.43\times10^7 N/m^2$. Figure 3-(b) shows a quarter model with a hole to obtain the finite difference sensitivity.

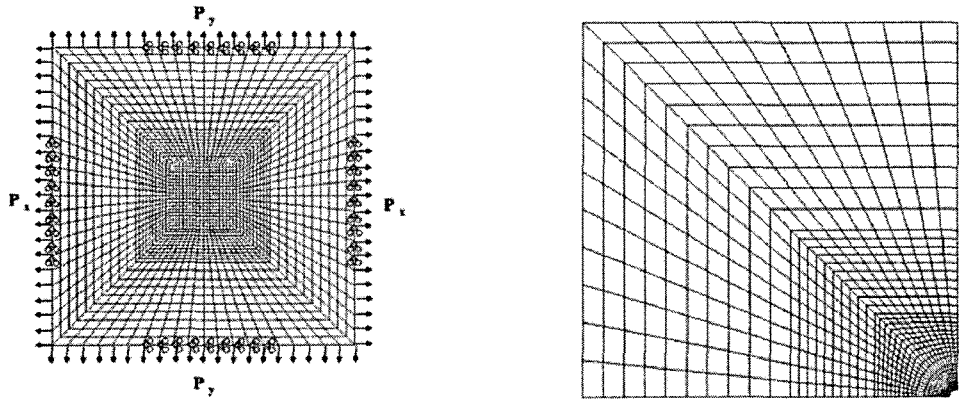

(a) Without hole (full model) (b) With hole (quarter model)

Figure 3 Verification model

In Table 1, the analytical design sensitivity coefficients of compliance computed from the developed method are compared with finite difference ones using the quarter model in Figure 3-(b). The columns of (a) and (b) stand for the analytical and the finite difference sensitivities, respectively. The finite difference sensitivity of compliance is obtained, using Equation (28), by

$$\dot{\psi}_T=\frac{\delta\psi(\Omega)}{\delta|\omega_\rho|}\cong\frac{\psi(\Omega_\rho)-\psi(\Omega)}{\delta|\omega_\rho|}, \tag{48}$$

The sensitivities are compared as reducing the radius of hole. In the last column, the agreement between analytical (a) and the finite difference (b) sensitivities are compared. The last column in Table 1 shows excellent agreements and improved results as reducing the radius of hole. When the radius is equal to 0.5, the best results are obtained.

Table 1 Comparison of compliance sensitivity

Radius	Compliance without hole	Compliance with hole	$\Sigma(z,\lambda)(\hat{x})$ (a)	Finite Difference Sensitivity (b)	(a) / (b) × 100 (%)
		Plane stress case			
1.50		3565.570		4923.928	94.45
1.20		3305.261		4816.591	96.56
0.95		3138.642		4746.896	97.98
0.70	2869.466	3013.999	4650.784	4694.525	99.07
0.50		**2942.594**		**4655.492**	**99.88**
0.30		2895.628		4626.452	100.53
0.10		2872.354		4596.018	101.18
0.02		2869.581		4570.226	101.76

Example 2: Nucleation amount

The objective of topological shape optimization is to obtain the optimal layout of structure, minimizing the compliance of structure and satisfying the requirement of allowable material volume. A simply supported plate model has the dimension of 1,800mm× 600mm, thickness of 10mm, Young's modulus of $E=2$ GPa, and Poisson's ratio of $\nu=0.3$ for plain stress problems and is subjected to a concentrated force of $F=1.0\times10^{7}N$.

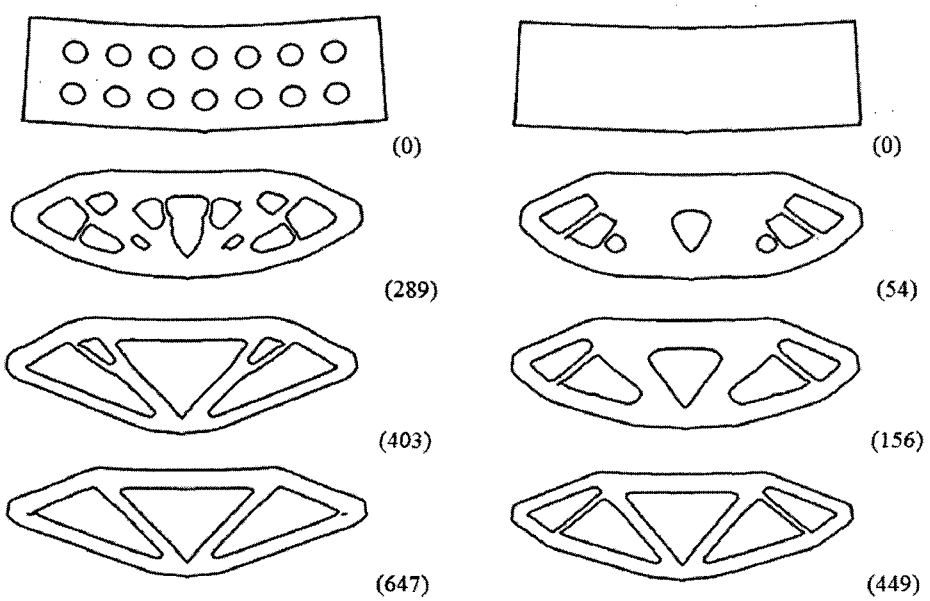

(a) **Case A**: without topological derivative (b) **Case B**: with topological derivative ($\beta=1.8$)

Figure 4 Comparison of design histories

Figure 4-(a) shows the history of implicit boundary obtained from the level set based optimization method. The design domain has the sufficient number of holes in the initial design and has no capability of nucleation (Case A). The number in the parenthesis denotes the iteration number. Figure 4-(b) shows the history without any holes inside the domain but incorporating the topological derivative for nucleation (Case B). In general, the shape optimization yields a local optimum which is strongly dependent on the initial design and consequently we obtain different optimal designs in Figure 4. In the Case A, if an initial model has no internal holes, the final optimal shape does not include any internal holes since the level set based optimization method never creates new internal holes. On the other hand, in the Case B, the level set based optimization method incorporating the topological derivative has the capability of nucleation.

The criterion for nucleation is obtained as

$$\dot{\Lambda}_T(\hat{\mathbf{x}}) = \dot{\psi}_T(\hat{\mathbf{x}}) + \beta\xi = -\Sigma(\mathbf{z},\boldsymbol{\lambda})(\hat{\mathbf{x}}) + \beta\xi \,, \tag{49}$$

where $\Sigma(\mathbf{z},\boldsymbol{\lambda})(\hat{\mathbf{x}})$ and ξ are non-negative quantities and β is a control parameter to speed up the optimization process. Whenever Equation (49) becomes negative, nucleation occurs at the point $\hat{\mathbf{x}}$. Once the topological variation occurs, *i.e.* nucleation, the other design variations are taken care of by the successive shape variations. The level set based optimization method using topological derivatives (Case B) yields faster convergent result than the existing level set based method (Case A).

7. CONCLUSIONS

A topological shape optimization method for linearly elastic structures is developed using the level set method and topological derivative approach. Since the implicit moving boundary is used, it is easy to represent the topological shape variations. Furthermore, there is no need to re-parameterize after significant shape changes during the optimization since the moving boundary is represented by implicit functions in the initial domain. Necessary design sensitivities are computed efficiently using the adjoint DSA method. Based on the asymptotic regularization concept, the topological derivative is considered as the limit of shape derivative as the radius of hole approaches to zero. For the optimization process, the required velocity field to integrate the Hamilton-Jacobi equation is obtained from Kuhn-Tucker optimality condition for the Lagrangian function. Numerical verification for the developed topological DSA method is performed by comparing the analytical sensitivity with the finite differencing, which shows very good agreement. The topological derivative is highly nonlinear with respect to the design variables. It also turns out that the initial holes in the domain is not required to get the optimal result since this method creates the holes during the optimization using the indicator obtained from the topological derivatives. It is demonstrated that the proper choice of the parameters β and n_{opt} is crucial for the efficiency of optimization process.

ACKNOWLEDGEMENTS

This work was supported by Advanced Ship Engineering Research Center of the Korea Science and Engineering Foundation (Grant Number R11-2002-104-06003-0) in 2005-2007. The support is gratefully acknowledged.

REFERENCES

1. S. Osher and J.A. Sethian, Front propagating with curvature dependent speed: algorithms based on Hamilton-Jacobi formulations, *Journal of Computational Physics* **79** (1988) 12-49.
2. G. Allaire, F. Jouve, and A. Toader, Structural optimization using sensitivity analysis and a level-set method, *Journal of Computational Physics* **194** (2004) 363-393.
3. S. Cho, S.H. Ha, and C.Y. Park, Topological Shape Optimization of Power Flow Problems at High Frequencies using Level Set Approach, *International Journal of Solids and Structures*, **43** (2006) 172-192.
4. S.H. Ha and S. Cho, Topological Shape Optimization of Heat Conduction Problems Using Level Set Method, *Numerical Heat Transfer Part B: Fundamentals*, **48** (2005), 67-88.
5. J. Kwak and S. Cho, Topological Shape Optimization for Geometrically Nonlinear Structures Using Level Set Method, *Computers and Structures* **83** (2005), 2257-2268.
6. J. Sokolowski, A. Zochowski, On topological derivative in shape optimization, SIAM Journal of Control and Optimization **37** (1999) 1251-1272.
7. Jean Céa, Stéphane Garreau, Philippe Guillaume, Mohamed Masmoudi, The shape and topological optimization connection, *Computer Methods in Applied Mechanics and Engineering* **188** (2000) 713-726.
8. A.A. Novotny, R.A. Feijóo, E. Tarroco, and C. Padra, Topological sensitivity analysis, *Computer Methods in Applied Mechanics and Engineering* **188** (2000) 713-726.